Environmental Pollution 324 (2023) 121343

Contents lists available at ScienceDirect

Environmental Pollution

journal homepage: www.elsevier.com/locate/envpol

Graphene oxide addition to anaerobic digestion of waste activated sludge: Impact on methane production and removal of emerging contaminants☆

Oriol Casabella-Font [a,b], Soraya Zahedi [a,c], Meritxell Gros [a,b], Jose Luis Balcazar [a,b], Jelena Radjenovic [a,d], Maite Pijuan [a,b,*]

[a] Catalan Institute for Water Research (ICRA), C. Emili Grahit 101, 17003, Girona, Spain
[b] Universitat de Girona, Girona, Spain
[c] Instituto de La Grasa, Spanish National Research Council (CSIC), Campus Universitario Pablo de Olavide– Ed. 46, Ctra. de Utrera, Km. 1, Seville, 41013, Spain
[d] Catalan Institution for Research and Advanced Studies (ICREA), Passeig Lluís Companys 23, 08010, Barcelona, Spain

ARTICLE INFO

Keywords:
Anaerobic treatment
Antibiotic resistance genes
Bio-reduced graphene oxide
Methane
Pharmaceuticals

ABSTRACT

The effect of graphene oxide on the anaerobic digestion of waste activated sludge was investigated at two graphene oxide concentrations (0.025 and 0.075 g graphene oxide per g volatile solids) using biochemical methane potential tests. The occurrence of 36 pharmaceuticals was monitored in the solid and liquid phases before and after the anaerobic treatment. The addition of graphene oxide improved the removal of most pharmaceuticals detected, even those that are considered persistent to biological degradation, such as azithromycin, carbamazepine, and diclofenac. No significant differences were observed in the final specific methane production without graphene oxide and with the lowest graphene oxide concentration, yet the highest graphene oxide concentration partially inhibited methane production. The relative abundance of antibiotic resistance genes was not affected by the graphene oxide addition. Finally, significant changes in the microbial community including bacteria and archaea were detected with graphene oxide addition.

1. Introduction

Since the early 2000s, many studies have reported the presence of pharmaceuticals in the secondary effluent from wastewater treatment plants (WWTPs) due to their incomplete removal by conventional activated sludge treatments (Barbosa et al., 2016; Gómez et al., 2007; Kümmerer, 2009; Spongberg & Witter, 2008). Moreover, and as a result of the constant presence of antibiotics, WWTPs are considered reservoirs of antibiotic resistant bacteria and antibiotic resistance genes (ARGs), where several groups of bacteria either contain ARGs or are potential hosts (Yun et al., 2021), being a threat to environmental health if discharged into the environment (Chen et al., 2019).

Waste activated sludge (WAS), which is produced in large quantities in WWTPs, contains a high concentration of these emerging pollutants. WAS is normally treated through anaerobic digestion (AD), a process that offers multiple advantages such as lower energy demands, sludge stabilization, and biogas production (Dai et al., 2017). For many years, hydrogen and formic acid transfer between methanogenic archaea and fermentative bacteria were assumed to be responsible for the transport of electrons, in a process known as indirect electron transfer (IET). The discovery of another thermodynamically more favorable route, direct interspecies electron transfer (DIET), opened up a whole new domain of opportunities for enhancing the performance of anaerobic processes (Summers et al., 2010; Wu et al., 2020). DIET is a cell-to-cell electron transfer between bacteria and methanogens via interspecies electrical connections: conductive pili and membrane-associated cytochromes. Given that the redox mediators are not required as electron shuttle, DIET overcomes the main limitation of IET related to the accumulation of volatile fatty acids (VFAs) and hydrogen, and inhibition of methanogens. DIET can be induced in methanogenic communities by adding conductive materials such as pyrolytic biochar, granular activated carbon (Johnravindar et al., 2020), Fe oxides-conductive carbon cloth (Fe_2O_3) (Y. Xu et al., 2020), and graphene-like materials (R. Lin et al., 2017; Muratçobanoğlu et al., 2022) to enhance biogas production of mixed anaerobic cultures (Lee et al., 2016; Rotaru et al., 2015; S. Xu et al., 2015). These conductive materials facilitate the electron exchange

☆ This paper has been recommended for acceptance by Su Shiung Lam.

* Corresponding author. Catalan Institute for Water Research (ICRA), C. Emili Grahit 101, 17003, Girona, Spain.
E-mail addresses: ocasabella@icra.cat (O. Casabella-Font), mpijuan@icra.cat (M. Pijuan).

https://doi.org/10.1016/j.envpol.2023.121343
Received 11 November 2022; Received in revised form 23 January 2023; Accepted 22 February 2023
Available online 7 March 2023
0269-7491/© 2023 The Authors. Published by Elsevier Ltd. This is an open access article under the CC BY-NC-ND license (http://creativecommons.org/licenses/by-nc-nd/4.0/).

among the different groups of microbes attached to them, thus facilitating the DIET process.

Graphene-based materials have attracted significant attention due to their remarkable chemical, electronic, structural, and mechanical properties (Zou et al., 2016). In the context of biological wastewater treatment, graphene oxide (GO) was reported to increase the ammonia removal by the anammox bacteria (D. Wang et al., 2013; G. Wang et al., 2014). There are also several studies on the GO addition to anaerobic digestion using different substrates (Dong et al., 2019; P. Wang et al., 2021), yet with contradictory findings regarding the impact on the methane production kinetics. Some studies report increasing biomethane yield and ARG removal when GO is added (Colunga et al., 2015; R. Lin et al., 2017; Zou et al., 2016). However, others indicate an inhibitory effect on the biomethane production (Dong et al., 2019; Zhang et al., 2017). Also, the impact of the GO on the occurrence of pharmaceuticals during anaerobic treatment of WAS has not been reported. This study investigates the impact of different GO concentrations on the anaerobic digestion of WAS. Batch tests were conducted to assess the maximum biogas production. The presence of a set of pharmaceutically active compounds (PhACs) was quantified in the solid and liquid matrices, in addition to the removal of ARGs at two different GO concentrations (0.025 and 0.075 g GO/g VS). Finally, analysis of the microbial community was also performed to identify possible changes in the bacteria and archaea caused by the addition of GO.

2. Materials and methods

2.1. Chemicals and sludge sources

GO was provided by Graphenea (Spain) as a 4 g/L aqueous dispersion, with a flake size <10 μm and elemental composition of 49–56% C, 0–1% H, 0–1% N, 2–4% S and 41–50% O. >95% of content was monolayer GO. PhACs and their isotopically labeled standards were purchased from Toronto Research Chemicals and Sigma-Aldrich.

WAS used as substrate and the inoculum were withdrawn from a local WWTP that treats municipal sewage (Girona, Spain) and that has an anaerobic digestion process operating at mesophilic conditions (35 °C). Table 1 summarizes the main characteristics of WAS and inoculum.

2.2. Biochemical methane potential tests

240 mL (100 mL working volume) glass serum bottles were used to carry out the biochemical methane production (BMP) tests, with an inoculum/substrate (I/S) of 2 (in VS) as detailed in Zahedi et al. (2018). Nitrogen gas was used to sparge each bottle before being sealed. BMP bottles were placed in a 35 °C incubator and shaken at 100 rpm to ensure mixing. Specific methane production (SMP) (mL CH_4/g VS) was reported at normal conditions (P = 1 atm and T = 273 K). Inoculum blank bottles were prepared to determine the endogenous methane production. All tests were conducted in triplicate, and the results are expressed as the mean with their standard deviations (SDs).

Three different tests were conducted in triplicate: *i)* control without addition of GO (Control), *ii)* addition of 0.025 g GO/g VS (GO_0.025), and *iii)* addition of 0.075 g GO/g VS (GO_0.075). GO was added according to the inoculum VS content. These GO concentrations were chosen because they were in the range of previous study that use the same substrate (Dong et al., 2019).

Table 1
Physicochemical properties of the inoculum and substrate (WAS) used in this study. Total solids (TS), volatile solids (VS), chemical oxygen demand (COD), biochemical oxygen demand (BOD), and total Kjeldahl nitrogen (TKN).

Parameter	Inoculum	WAS
pH	7.68 ± 0.09	6.82 ± 0.06
tCOD (mg O_2/L)	21,600 ± 200	26,850 ± 250
$tBOD_5$ (mg O_2/L)	1976 ± 80	2527 ± 139
TS (g/L)	22.22 ± 0.11	23.39 ± 0.16
VS (g/L)	14.36 ± 0.08	17.38 ± 0.11
PO_4^{3-}P (mg/L)	12.35 ± 0.02	8.2 ± 0.03
PT (mg/L)	458.85 ± 7.16	343.91 ± 21.06
Cl^- (mg/L)	237.87 ± 0.10	158.18 ± 0.10
Na^+ (mg/L)	117.11 ± 0.02	126.07 ± 0.06
NH_4^+-N (mg/L)	891.48 ± 10.35	216.02 ± 14.55
TKN (mg/L)	2004 ± 30	1726 ± 39

2.3. Methane production modeling

To investigate the impact of GO on AD, two kinetic parameters were determined using the model proposed by Dong et al. (2019): hydrolysis rate (k), and biochemical methane production potential (M_0). To estimate the numerical value, the experimental data obtained in the tests was adjusted to a first-order kinetic model with the sum squared errors as the objective function. The first-order kinetics equation used was (Eq. (1)):

$$M(t) = M_0 \cdot \left(1 - e^{-kt}\right) \quad (1)$$

where daily methane production is $M(t)$ (mL CH_4/g VS), biochemical methane production potential is M_o (mL CH_4/g VS), and hydrolysis rate is k (d^{-1}) (hydrolysis is considered as the rate-limiting step in AD with complex substrates (Batstone et al., 2009)), and t is time (d) (Dong et al., 2019; Y. Liu et al., 2015). ANOVA test was done using Minitab 17 Statistical Software (State College, PA: Minitab, Inc.) to check the statistically significant differences in the experimental results.

2.4. Analytical methods

Total solids (TS), volatile solids (VS), chemical oxygen demand (COD), biochemical oxygen demand (BOD), and total Kjeldahl nitrogen (TKN) were quantified as described in APHA (2017); Alvarino et al. (2014). Volatile fatty acids (VFAs) were quantified with gas chromatography (Trace GC Ultra ThermoFisher Scientific), and cations and anions were quantified with ion chromatography (ICS5000, DIONEX).

Methane composition in the headspace was determined with an infrared CH_4 sensor (GasTech S-Guard). Biogas production was monitored using a pressure sensor (PM7097, IFM) measuring the pressure in the headspace of each BMP bottle before sampling.

2.4.1. Pharmaceuticals extraction and quantification

The set of 36 target pharmaceuticals was analyzed in the liquid and solid fractions in duplicate, and the results are expressed as mean with their SDs. The analysis of the solid fraction included the initial inoculum and WAS used as the substrate, and the samples from the end of the tests (after 33 days of anaerobic digestion). The solid fraction samples were freeze-dried (−82 °C and 0.033 bar) and extracted with citric acid and acetonitrile (Gros et al., 2019b; Zahedi et al., 2021). After that, the extracts were purified by solid phase extraction (SPE) using Oasis Accell™ Plus QMA (500 mg, 6 mL) and Oasis HLB (200 mg, 6 mL) cartridges, operating in tandem, according to a previously developed method (Gros et al., 2019a). The liquid fraction analysis included supernatant before and after the BMP tests, which was filtered and preconcentrated by SPE using Oasis HLB (200 mg, 6 mL) cartridges. Total concentrations of pharmaceuticals were calculated using equation (2).

$$C_{total} = C_{liquid} + C_{solid} \cdot \%TS_{solid\ fraction} \cdot g_p / g_l \quad (2)$$

where the pharmaceutical concentrations are C_{liquid} and C_{solid} detected respectively in the liquid and solid (lyophilized) fraction. $_p$ and g_l are the weights of the solid fraction (pellet) and liquid fraction before centrifugation, and the solid fraction (%TS) was calculated as the ratio of the pellet weight after being freeze-dried and pellet weight previously being freeze-dried.

WAS and inoculum were analyzed separately at the beginning of the experiment and the concentrations of each pharmaceutical at initial time were calculated as follows (Eq. (3)):

$$C_{BMP\ intial} = (C_{inoculum} \cdot V_{inoculum}) + (C_{WAS} \cdot V_{WAS}) / (V_{inoculum} + V_{WAS}) \quad (3)$$

where $C_{inoculum}$ and C_{WAS} are the concentrations of the pharmaceuticals in the inoculum and WAS, and $V_{inoculum}$ and V_{WAS} are the volumes of inoculum (62.42 mL) and WAS (25.75 mL) added in each BMP test, respectively.

Samples were analyzed in duplicate using an Acquilty Ultra-High Performance-Liquid chromatography (UHPLC) system (Waters Corporation, MA, USA) in tandem with a 5500 QTRAP hybrid quadrupole-linear ion trap mass spectrometer (AB Sciex, Foster City, USA). Matrix interferences were corrected using isotopically labeled standards, and recoveries (Table S1), and physicochemical properties are defined in Table S2 for each compound. Removal efficiencies (%) were calculated using the difference in the total concentration for each condition (Eq. (3)) at the beginning and the end of the experiment.

2.4.2. DNA extraction and characterization

FastDNA™ SPIN Kit for Soil (MP Biomedicals, USA) was used to extract the DNA from the microbial samples. This extraction was done in duplicate, for WAS and inoculum samples before their addition to the BMP bottles and after mixing, and for the solid fraction from the end of the anaerobic treatment. Five ARGs were analyzed by real-time PCR (qPCR). The selection of ARGs was done according to their clinical and environmental relevance, including those conferring resistance to the main antibiotic families used to treat bacterial infections, namely: carbapenems (blaKPC), fluoroquinolones (qnrS), macrolide-lincosamide-streptogramin antibiotics (ermB), sulfonamides (sul1) and tetracyclines (tetW). The *intI 1* gene was also monitored as a proxy for anthropogenic pollution and horizontal gene transfer, as previously described (Subirats et al., 2017). Primers used and qPCR parameters are summarized in Table S3 (Supplementary material). For all qPCR assays, a CFX96 Thermal cyclers system (Biorad, Hercules, USA) was used to perform dissociation curves (from 60 °C to 95 °C). ANOVA test was done by using Minitab 17 Statistical Software (State College, PA: Minitab, Inc.), to check the statistically significant differences among the experimental results. Illumina MiSeq platform from Macrogen Inc. (Seoul, South Korea) was used to characterize the bacteria and archaea microbial community using high-throughput sequencing of the 16 S rRNA gene. Analysis of 16 S rRNA gene sequences was performed using the MOTHUR software package (Schloss et al., 2009).

3. Results

3.1. Impact of graphene oxide on biogas production

The SMP production of WAS assessed under different concentrations of GO and the results are presented in Fig. 1. Methane production was monitored for 33 days, reaching 196 ± 8, 198 ± 7, and 158 ± 7 mL CH_4/g VS in the control, 0.025 g GO/gVS, and 0.075 g GO/gVS, respectively. ANOVA (two-ways) test confirmed no significant ($p > 0.05$) differences between control and GO_0.025 cumulative SMP but found significant differences ($p < 0.05$) with the cumulative SMP in the experiment GO_0.075. Specifically, SMP decreased by 19 ± 3% at the dosage of 0.075 g GO/g VS in comparison with the control.

The kinetic model (first order) proposed by Dong et al. (2019) (Eq. (1)) was applied to simulate the BMP tests with different GO dosing, obtaining the two kinetic parameters used for comparison: *k*, and M_0. Table 2 summarizes the experimental SMP and kinetic parameters calculated for each condition. The results are also depicted in Fig. 1, showing a satisfying fitting between the experimental data and model simulation. The coefficient of determination (R^2) was >0.99 for all conditions.

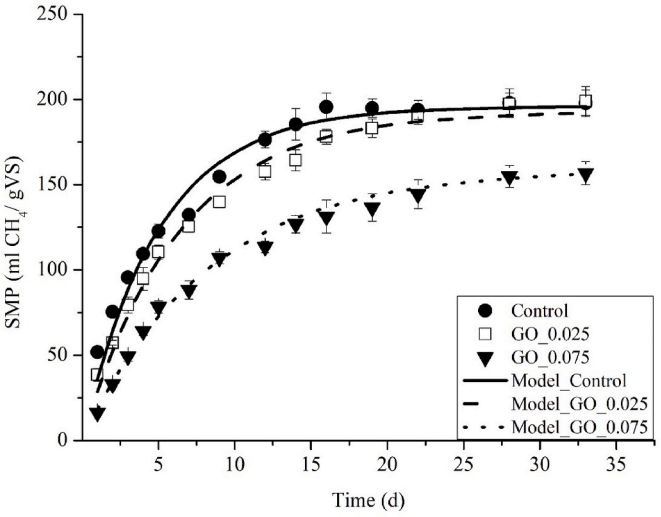

Fig. 1. Cumulative specific methane production (SMP) with standard deviation for experimental data and model curve at different graphene oxide (GO) concentrations; (●) 0 g GO/g VS; (□) 0.025 g GO/g VS; (▼) 0.075 g GO/g VS.

Table 2
Summary of the experimental SMP and kinetic parameters calculated for each condition studied.

GO concentration (g GO/g VS)	Max. SMP (mL CH_4/g VS)	Hydrolysis rate *k* (d^{-1})	Biochemical Methane potential M_0 (mL CH_4/g VS)	Correlation Exp-Model
Control	196.0 ± 7.7	0.202 ± 0.011	195.9 ± 7.7	0.990 ± 0.002
GO_0.025	198.1 ± 6.9	0.161 ± 0.009	193.0 ± 6.2	0.995 ± 0.001
GO_0.075	158.5 ± 6.8	0.123 ± 0.004	159.1 ± 8.5	0.996 ± 0.002

The estimated M_0 values showed no significant differences ($p > 0.05$) between maximum SMP obtained with Control and GO_0.025, but significant differences ($p < 0.05$) were observed when compared with GO_0.075. However, *k* showed significant differences ($p < 0.05$) among all conditions studied. Compared with the Control without GO, a reduction of 21% ± 4% for 0.025 g GO/g VS, and 39% ± 2% for 0.075 g GO/g VS was detected for the *k* parameter, indicating that GO had a negative impact on the hydrolysis step of the process.

Dong et al. (2019) obtained similar results and suggested that the reduction in maximum methane production and the kinetic rate was caused by the negative effect of GO over the hydrolysis and methanogenesis steps because of the adsorption capability of GO on soluble proteins and carbohydrates. The same study found a biomethane reduction of 7.6% and 12.6% at 0.054 and 0.104 g GO/g VS using WAS as substrate. In another study, methane production was decreased by 13% in AD of swine manure (5 mg GO/L) (Zhang et al., 2017). Since no accumulation of VFA (soluble COD) was detected at the end of the batch test in the current study, and assuming that any possible adsorbed organic matter would be consumed by the microorganisms, slower kinetics of methane production are likely a consequence of the electron scavenging by the GO bioreduction. The bioreduction process of GO consists of the anaerobic reduction of the oxygen functional groups (see Section 2.1) present in the nanomaterial structure. Supplying electrons to this initial reduction of GO implies a reduction of electrons that can be used for methane production, thus resulting in a reduction of the kinetic constant (*k*) as observed in this study. Furthermore, a recent study (Ponzelli et al., 2022) showed that in a substrate fed-batch strategy,

when the second substrate pulse was added an anaerobic sludge supplemented with GO (bio-rGO), methane production as well as the kinetic parameters (M_0 and k) were increased, reaching SMP values similar as the control without GO. This is a strong indication that the initial biological reduction of GO causes a decrease in the methane yield.

3.2. Impact of graphene oxide on the removal of pharmaceuticals

After an initial screening, 17 out of the 36 compounds analyzed were detected in the inoculum and WAS used at the beginning of the experiment (Table 3). Given that both WAS and inoculum were obtained from the same WWTP, the presence and abundance of pharmaceuticals were similar for these two fractions. Only three compounds (ibuprofen, losartan, and valsartan) were more ubiquitous in the inoculum liquid phase, whereas clarithromycin and venlafaxine were mostly detected in the WAS liquid matrix. As demonstrated by Gros et al., 2019a, there was no correlation between pharmaceuticals sorption to the solid phase in a biological process and their hydrophobicity, indicated by their LogD values, a parameter widely used to measure hydrophobicity of ionizable compounds, dependent on the pH. Previous studies associated the presence of pharmaceuticals in the sludge with their tendencies for electrostatic interactions (Senta et al., 2011; W. Xu et al., 2007). Although fluoroquinolone antibiotics (ciprofloxacin, ofloxacin, and norfloxacin) have low logD values (−2.08 to −3, Table S2), they were present in higher concentrations in the solid fraction of the inoculum and WAS compared with more hydrophobic pharmaceuticals such as carbamazepine, losartan, and diclofenac (LogD from 1.29 to 2.28, Table S2), which were mostly detected in the liquid fraction.

Average concentrations considering liquid and solid phases (calculated with Eq. (2)) for each compound at the initial time (t = 0 d) and after anaerobic treatment (t = 33 d) are shown in Fig. 2A, and removal efficiencies are presented in Fig. 2B. Data presented in Table 3 show the concentration for each compound detected in the liquid and the solid phase.

In general, the addition of GO had a positive effect on the removal of most antibiotics. Compounds were classified into three categories according to their fate during the BMP tests (Fig. 2B): i) pharmaceuticals showing enhanced removal at any GO concentration, ii) pharmaceuticals with enhanced removal only at the highest GO concentration tested, and *iii)* pharmaceuticals with lower removal at any GO concentration. It should be noted here that due to the determination of target pharmaceuticals in both liquid and solid fractions of the sampled sludge, and isotopically labeled standards were used, their removal was most likely linked to anaerobic biotransformation.

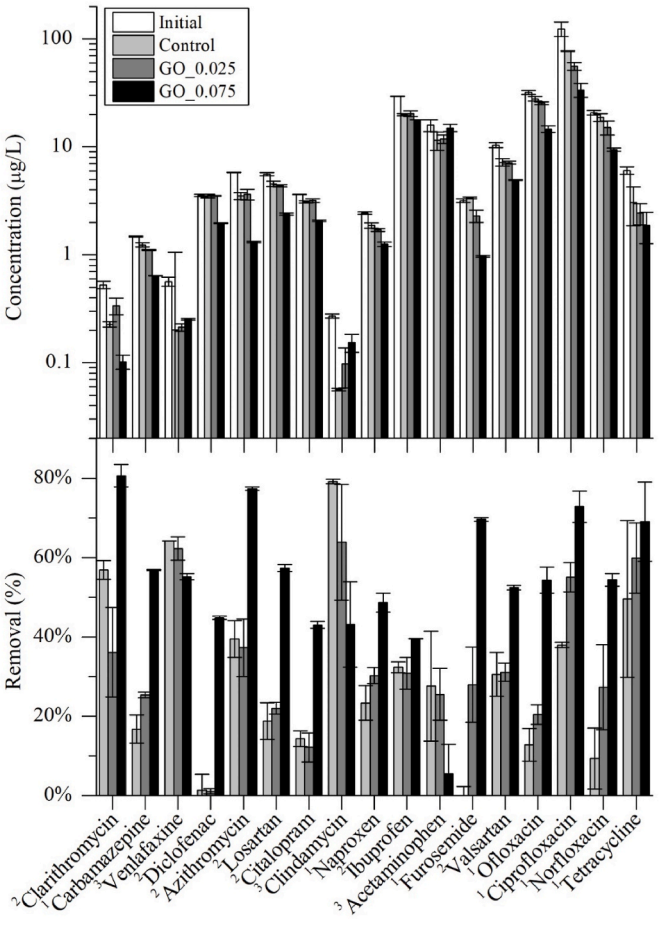

Fig. 2. (A) Total pharmaceutical concentrations before and after the anaerobic treatment at different GO concentrations. (B) Removal efficiencies for each compound obtained in anaerobic treatment. Ordered by LogD value. 1 Enhanced removal at any GO concentration. 2 Enhanced removals only at the highest GO concentration. 3 Negative effect of GO on the removal efficiency.

Of the 17 pharmaceuticals detected, 14 compounds exhibited an enhanced removal with GO addition (seven at any GO concentration and

Table 3
Pharmaceuticals detected in the liquid and solid fractions from WAS and inoculum and at the end of the BMP tests.

Compound	WAS		Inoculum		Control		GO_0.025		GO_0.075	
	Solid (µg/kg)	Liquid (µg/L)	Solid (µg/kg)	Liquid (µg/L)	Solid (µg/kg)	Liquid (µg/L)	Solid (µg/kg)	Liquid (µg/L)	Solid (µg/kg)	Liquid (µg/L)
Acetaminophen	0.98 ± 0.06	0.20 ± 0.02	0.79 ± 0.13	0.95 ± 0.13	0.69 ± 0.15	1.71 ± 0.09	0.68 ± 0.05	1.55 ± 0.27	1.08 ± 0.09	0.83 ± 0.03
Azithromycin	0.24 ± 0.03	0.31 ± 0.02	0.33 ± 0.01	0.25 ± 0.35	0.25 ± 0.02	0.00 ± 0.00	0.24 ± 0.03	0.00 ± 0.00	0.10 ± 0.00	0.00 ± 0.00
Carbamazepine	0.02 ± 0.00	0.64 ± 0.01	0.03 ± 0.00	1.48 ± 0.01	0.03 ± 0.00	0.82 ± 0.03	0.03 ± 0.00	0.59 ± 0.02	0.03 ± 0.00	0.19 ± 0.00
Ciprofloxacin	7.24 ± 0.07	0.65 ± 0.02	6.66 ± 1.50	1.13 ± 0.08	5.39 ± 0.06	0.79 ± 0.00	3.70 ± 0.31	0.27 ± 0.06	2.57 ± 0.38	0.00 ± 0.00
Citalopram	0.13 ± 0.00	0.03 ± 0.00	0.23 ± 0.00	0.06 ± 0.02	0.22 ± 0.01	0.00 ± 0.00	0.21 ± 0.01	0.00 ± 0.00	0.16 ± 0.00	0.00 ± 0.00
Clarithromycin	0.07 ± 0.00	0.06 ± 0.00	0.01 ± 0.00	0.03 ± 0.00	0.01 ± 0.00	0.04 ± 0.00	0.02 ± 0.00	0.01 ± 0.00	0.01 ± 0.00	0.00 ± 0.00
Clindamycin	0.02 ± 0.00	0.13 ± 0.02	0.01 ± 0.00	0.08 ± 0.01	0.00 ± 0.00	0.00 ± 0.00	0.01 ± 0.00	0.01 ± 0.02	0.01 ± 0.00	0.02 ± 0.00
Diclofenac	0.14 ± 0.01	2.13 ± 0.04	n.d.	3.90 ± 0.20	0.10 ± 0.00	2.12 ± 0.11	0.11 ± 0.00	1.84 ± 0.03	0.09 ± 0.00	0.73 ± 0.01
Furosemide	0.04 ± 0.00	2.06 ± 0.09	0.04 ± 0.01	3.22 ± 0.06	0.04 ± 0.00	2.78 ± 0.03	0.05 ± 0.00	1.60 ± 0.24	0.04 ± 0.00	0.39 ± 0.02
Ibuprofen	0.10 ± 0.00	3.54 ± 0.11	0.25 ± 0.02	41.60 ± 0.28	0.16 ± 0.00	17.58 ± 0.45	0.23 ± 0.04	16.90 ± 0.59	0.22 ± 0.00	14.88 ± 0.06
Losartan	0.03 ± 0.00	0.71 ± 0.02	0.08 ± 0.00	7.01 ± 0.27	0.07 ± 0.00	3.50 ± 0.28	0.11 ± 0.01	2.70 ± 0.06	0.10 ± 0.00	1.01 ± 0.04
Naproxen	0.02 ± 0.01	1.36 ± 0.00	0.05 ± 0.00	2.21 ± 0.07	0.06 ± 0.00	1.04 ± 0.06	0.05 ± 0.01	0.92 ± 0.04	0.04 ± 0.00	0.74 ± 0.06
Norfloxacin	0.83 ± 0.09	n.d.	1.25 ± 0.04	0.32 ± 0.09	1.33 ± 0.11	0.00 ± 0.00	1.00 ± 0.15	0.00 ± 0.00	0.72 ± 0.03	0.00 ± 0.00
Ofloxacin	1.58 ± 0.12	0.28 ± 0.01	1.82 ± 0.06	0.34 ± 0.03	1.95 ± 0.09	0.26 ± 0.01	1.68 ± 0.05	0.15 ± 0.00	1.11 ± 0.08	0.09 ± 0.00
Tetracycline	0.28 ± 0.04	0.11 ± 0.02	0.35 ± 0.02	0.16 ± 0.02	0.21 ± 0.09	0.07 ± 0.00	0.16 ± 0.04	0.04 ± 0.01	0.14 ± 0.05	0.02 ± 0.00
Valsartan	0.04 ± 0.01	1.20 ± 0.07	0.08 ± 0.00	14.96 ± 0.90	0.06 ± 0.00	6.36 ± 0.62	0.08 ± 0.00	5.97 ± 0.18	0.10 ± 0.01	3.65 ± 0.13
Venlafaxine	0.04 ± 0.00	0.30 ± 0.00	0.02 ± 0.00	n.d.	0.01 ± 0.00	0.00 ± 0.00	0.01 ± 0.00	0.00 ± 0.00	0.02 ± 0.00	0.00 ± 0.00

seven only at the highest GO concentration (Fig. 2B)). The addition of GO facilitated the removal of azithromycin and clarithromycin achieving removal efficiencies of around 80% with the highest GO concentration (0.075 g GO/gVS). These two compounds typically present around 50% removal under standard anaerobic digestion conditions (Feng et al., 2017; Narumiya et al., 2013; Zahedi et al., 2021), in accordance with what was also found in the Control BMP tests i.e., 40% and 60% removals, respectively.

Furosemide, diclofenac, and carbamazepine were the three compounds with the highest enhancement of its removal when GO was added. Their removal in the BMPs without the GO addition was almost negligible (0%, 1.3%, and 16.7%, respectively) and was substantially increased with GO addition to 69.7%, 44.8%, and 56.9%, respectively, at the highest GO concentration tested. Indeed, several studies reported poor removal (<20%) of these compounds in the anaerobic treatment (Alvarino et al., 2014; Bergersen et al., 2012; Falås et al., 2016; Gonzalez-Gil et al., 2017; Lahti & Oikari, 2010; K. Lin & Gan, 2011; Narumiya et al., 2013; Xue et al., 2010), which is in agreement with the results obtained in the BMPs without GO addition.

Norfloxacin and ofloxacin exhibited ~10% removal under anaerobic conditions without GO. Their removal increased substantially when GO was added, achieving 54% removal at the highest GO concentration tested. Previous studies demonstrated that fluoroquinolone antibiotics are hardly degraded under anaerobic conditions (Golet et al., 2003). Also, losartan and valsartan showed similar behavior and enhanced removal rates were observed only at the highest GO concentration tested. For Control and GO_0.025, losartan presented 20% removal and valsartan ~30%. However, in the GO_0.075 tests, the removal was increased to 57% for losartan and 52% for valsartan.

Of the 17 pharmaceuticals detected, only acetaminophen, clindamycin, and venlafaxine exhibited inhibition in their biotransformation in the presence of GO, and the decrease in their removal efficiencies was more pronounced at the highest GO concentrations, showing reductions of 23%, 36%, and 9%, respectively. Regarding their presence in different phases, lower concentrations were found in the liquid phase with the addition of GO for these three compounds (Table 3).

3.3. Impact of graphene oxide addition on the microbial community

Alfa (α) diversity values of the microbial community were calculated for the initial mixture and after treatment without GO (Control) and 0.075 g GO/g VS. Results were presented separately for bacteria and archaea in Table S3. The original mixture and the two treatments had a similar number of operational taxonomic units (OTUs) in both bacteria and archaea. Higher diversity and richness were observed at GO_0.075, as indicated by a higher Shannon diversity index for bacteria (5.82 ± 0.02) and archaea (2.62 ± 0.02), in comparison with the Control (5.39 ± 0.19 and 1.87 ± 0.04, respectively).

At phylum level, Actinobacteria reduced their presence to 5% at GO_0.075 replicates (from 35% in the baseline condition, Fig. S1). On the other hand, Proteobacteria benefited from the presence of GO and reached a relative abundance of 21% at the end of the GO_0.075 test.

Fig. 3A shows the heatmap of the most abundant bacterial genera present in the samples analyzed, and the impact of GO addition. Bacterial genera such as *Romboutsia* (Firmicutes), *Longilinea* and *Candilinea* (Chloroflexi), and *Hyphomicrobium* (Proteobacteria) seemed to have been favored by the addition of GO, while *Microthrix*, *Phycicoccus* (Actinobacteria) and *Sedimentibacter* (Firmicutes) showed lower relative abundance in the effluent containing GO.

Regarding the Archaea domain, Euryarchaeota was the most abundant phyla (>95%) in all samples. Significant differences were observed (Fig. 3B) in the samples with and without GO. The most abundant genera in the Control effluent (GO_0) were acetoclastic methanogens such as *Methanosaeta* spp. And *Methanosaetaceae* spp. However, in the GO_0.075 effluent, the most abundant genera were hydrogenotrophic methanogens such as *Methanobacterium* spp., *Methanosarcina* spp., *Methanomassiliicoccus* spp., *Methanospirillum* spp. And *Methanobrevibacter* spp.

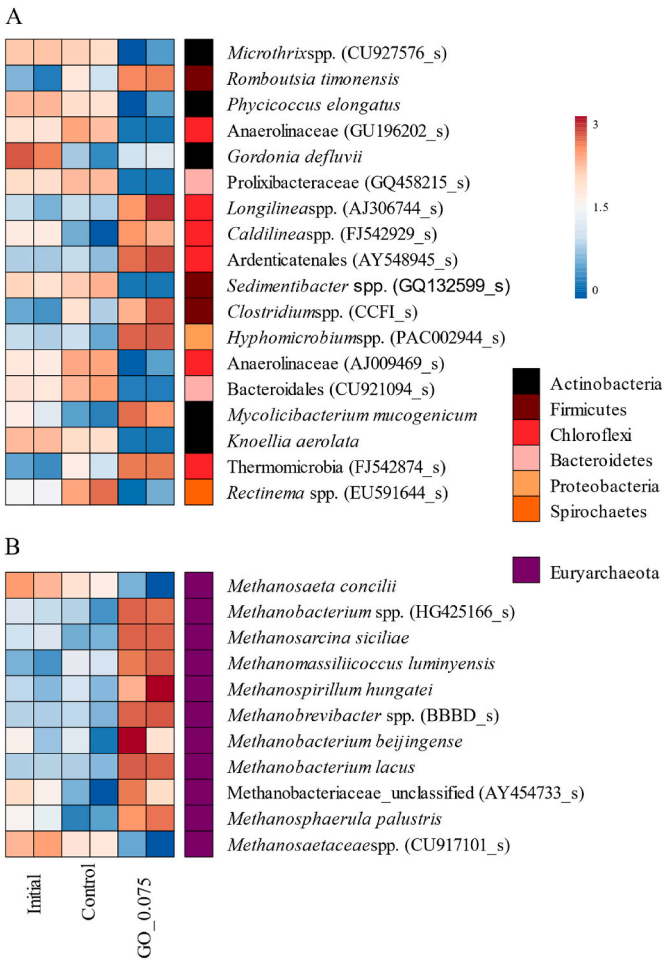

Fig. 3. Heatmap of the most abundant bacterial (A) and archaeal (B) genera (or species) found in the initial mix, and after conventional anaerobic treatment with and without GO addition.

The main difference in the microbial community with and without GO addition was observed in archaea, showing a completely different promotion of methanogens after the treatment. At the end of the experiment for the control conditions, acetoclastic methanogens were more present in comparison with hydrogenotrophic methanogens. On the other hand, after the treatment with GO, an increment of the hydrogenotrophic community was detected in comparison with acetoclastic archaea. This finding suggests that GO might promote those archaea groups which use hydrogen and CO_2 as substrates, to detriment of those that use organic molecules such as acetic acid. Li et al. (2016) reported an enriched culture of hydrogenotrophic methanogens over a graphite electrode in a microbial electrochemical cell. In another study, the addition of GAC enhanced the presence of hydrogenotrophic methanogens, such as *Methanospirillum* spp. (Lee et al., 2016). In the present study, the same genus was enriched after the treatment with GO, suggesting that GO can be used by those microorganisms which produce CH_4 from hydrogen and CO_2.

3.4. Relative abundance of antibiotic resistance genes

Three out of five ARGs analyzed (*sul1, ermB, and tetW*), together with the *intl1* genes were detected in the inoculum, WAS, and the anaerobic effluents, and the results are presented in Fig. 4. Two of the target ARGs, bla_{KPC} and *qnrS*, were below the quantification limit (11 and 54 copies, respectively).

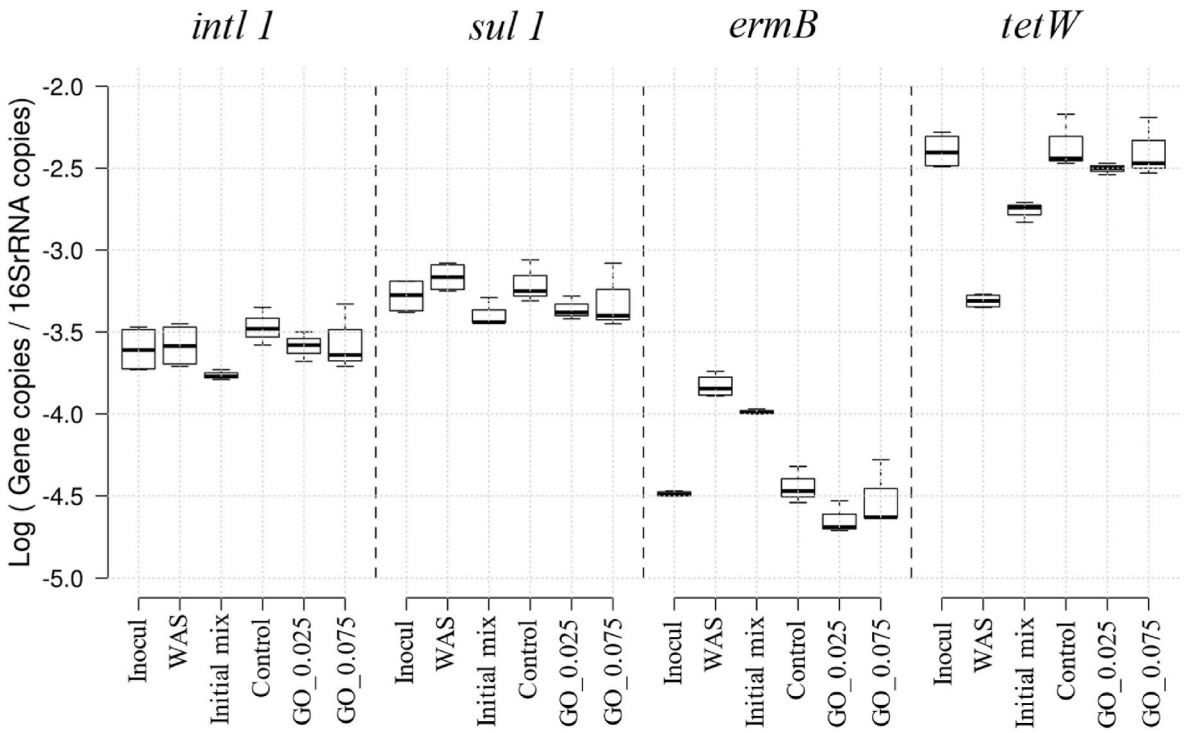

Fig. 4. Presence of antibiotic resistance genes in the inoculum and WAS used, at the beginning of the BMPs (Initial), and after 33 days of anaerobic treatment with different GO concentrations.

When looking at the inoculum, the gene *tetW* was the most abundant, while *ermB* showed the lowest abundance. The *sul1* gene which confers resistance to sulfonamides and the *intl1* gene presented similar abundances between the anaerobic inoculum and WAS. Regarding the anaerobic effluents, no significant differences ($p > 0.05$) were found at the end of the BMPs conducted at different GO concentrations.

There are different studies published in the literature that assessed the impact of GO on the removal of ARG. Physical absorption is the main removal mechanism of GO for ARG removal and can reduce the horizontal gene transfer of ARG located in plasmids (Bytesnikova et al., 2021; Wei & Ge, 2013; Zou et al., 2016). Different bacteria phylum, such as Firmicutes, Bacteroidetes, and Spirochaetes, had been correlated to the presence of ARG during the anaerobic digestion process of swine manure with GO (100 and 800 mg/L) (R. Zhang et al., 2019, 2022). The results obtained in the present study showed that phylum increased its relative abundance in presence of GO (see section 3.1.). In the present study, the gene *ermB* was the only one that reduced its relative abundance. Previous studies (P. Wang et al., 2021; J. Zhang et al., 2017) reported that the anaerobic digestion process could reduce the abundance of that gene after the addition of GO. This result is by what was obtained in the present study. The same studies also reported the reduction of the genes *sulI*, *tetW*, and *IntI1* by the addition of 5 and 500 mg/L of GO, contrary to what was obtained in this study.

3.5. Improving anaerobic pharmaceutical removal through GO addition: possible mechanisms

Concerning the removal of pharmaceuticals, results obtained in the presence of GO showed that this nanomaterial could enhance the biological transformation for most of the compounds reported in the present study (14 out of 17 compounds detected). GO has multiple oxygen functional groups (e.g. epoxy, carbonyl) in its structure, and carboxyl groups at the edges (Aliyev et al., 2019; Alvarino et al., 2014). Most of the compounds that increased their removal when exposed to any concentration of GO presented carboxyl functional groups in their structure (Table S2). The biological transformation of the pharmaceuticals could be linked with the gene expressed during the biological reduction of GO, enhancing the removals in presence of GO. On another note, a change in the microbial population was detected in the present study as certain microorganisms can utilize the electrons present in the conductive material to thrive. The proliferation of hydrogenotrophic methanogens demonstrated that syntrophic micromicroorganisms use the electron that flows through the GO structure. Also, at the bacterial level, some genera (belonging to Firmicutes and Chloroflexi phylum) were promoted in the detriment of others. Firmicutes were reported as the predominant phyla in the anode of a microbial fuel cell (>80% relative abundance), implying their functional role in current production (Wrighton et al., 2008). One possible mechanism for the biotransformation of the pharmaceuticals detected in the present study could be the impact of a conductive material such as bio-rGO, acting as a conductive material for electrons, thus enhancing the flow of electrons available for the microorganisms to transform some organic micropollutants as was previously reported by Colunga et al. (2015). Further research is on the way to verify some of the hypothesis presented.

4. Conclusions

In the present study, the impact of GO on methane production and pharmaceutical compound removal was assessed. The main conclusions are the following.

- The addition of 0.025 g GO/gVS did not affect the specific methane production of WAS, but a reduction of 19% was observed in the presence of 0.075 g GO/gVS. For both conditions, a decrease in the kinetic constant was detected.
- PhACs elimination during anaerobic digestion from the whole matrix (liquid and solid phases) significantly increased for most of the compounds detected with the highest GO concentration.
- The addition of GO did not have an impact on the relative abundance of target ARGs within the range of concentrations tested.

- GO had an effect on microbial population diversity, enhancing the abundance of hydrogenotrophic archaea and to detriment of aceto-clastic methanogens.

The results of this study revealed GO as an alternative to other carbon-based materials used in the anaerobic digestion process to enhance the removal of pharmaceuticals. However, more studies with kinetic monitoring of the desired compound are needed to identify the transformation mechanisms for each compound's transformation product identification.

Credit author statement

Oriol Casabella: Methodology, Investigation, Writing - Original Draft, **Soraya Zahedi:** Investigation, Writing - Review & Editing, **Meritxell Gros:** Resources, Writing - Review & Editing, **Jose Luís Balcazar:** Formal analysis, Writing - Review & Editing, **Jelena Radjenovic:** Methodology, Writing - Review & Editing, Funding acquisition, **Maite Pijuan:** Methodology, Writing - Review & Editing, Funding acquisition.

Data-availability

Data will be made available on request.

Declaration of competing interest

The authors declare that they have no known competing financial interests or personal relationships that could have appeared to influence the work reported in this paper.

Data availability

Data will be made available on request.

Acknowledgments

This research is funded by AEI (*Agencia Estatal de Investigación*, Spanish Government) through project ANTARES (PID 2019-110346RB-C22). O. Casabella acknowledges funding from the Secretariat of Universities and Research from Generalitat de Catalunya and the European Social Fund for his FI fellowship (2022 FI_B1 00122). M. Gros acknowledges her Ramon y Cajal contract (RYC 2020-030324-I) funded by the MCIN/AEI 10.13039/501100011033 and by "ESF Investing in your future". The authors acknowledge the support from the Economy and Knowledge Department of the Catalan Government through a Consolidated Research Group (ICRA-TECH - 2021 SGR 01283) and (SGR ICRA-ENV 2021 01282).

References

Aliyev, E., Filiz, V., Khan, M.M., Lee, Y.J., Abetz, C., Abetz, V., 2019. Structural Characterization of Graphene Oxide: Surface Functional Groups and Fractionated Oxidative Debris. Nanomaterials 9 (1180), 1–15. https://doi.org/10.3390/nano9081180.

Alvarino, T., Suarez, S., Lema, J.M., Omil, F., 2014. Understanding the removal mechanisms of PPCPs and the influence of main technological parameters in anaerobic UASB and aerobic CAS reactors. J. Hazard Mater. 278, 506–513. https://doi.org/10.1016/j.jhazmat.2014.06.031.

APHA, 2017. Standard Methods for the Examination of Water and Wastewater. Federation. Water Environmental American Public Health Association (APHA), Washington, DC, USA.

Barbosa, M.O., Moreira, N.F.F., Ribeiro, A.R., Pereira, M.F.R., Silva, A.M.T., 2016. Occurrence and removal of organic micropollutants: an overview of the watch list of EU Decision 2015/495. Water Res. 94, 257–279. https://doi.org/10.1016/j.watres.2016.02.047.

Batstone, D.J., Tait, S., Starrenburg, D., 2009. Estimation of hydrolysis parameters in full-scale anerobic digesters. Biotechnol. Bioeng. 102 (5), 1513–1520. https://doi.org/10.1002/bit.22163.

Bergersen, O., Hanssen, K.Ø., Vasskog, T., 2012. Anaerobic treatment of sewage sludge containing selective serotonin reuptake inhibitors. Bioresour. Technol. 117, 325–332. https://doi.org/10.1016/j.biortech.2012.04.086.

Bytesnikova, Z., Adam, V., Richtera, L., 2021. Graphene oxide as a novel tool for mycotoxin removal. Food Control 121, 20148–20163. https://doi.org/10.1016/j.foodcont.2020.107611.

Chen, Y., Su, J.Q., Zhang, J., Li, P., Chen, H., Zhang, B., Gin, K.Y.H., He, Y., 2019. High-throughput profiling of antibiotic resistance gene dynamic in a drinking water river-reservoir system. Water Res. 149, 179–189. https://doi.org/10.1016/j.watres.2018.11.007.

Colunga, A., Rangel-Mendez, J.R., Celis, L.B., Cervantes, F.J., 2015. Graphene oxide as electron shuttle for increased redox conversion of contaminants under methanogenic and sulfate-reducing conditions. Bioresour. Technol. 175, 309–314. https://doi.org/10.1016/j.biortech.2014.10.101.

Dai, X., Xu, Y., Dong, B., 2017. Effect of the micron-sized silica particles (MSSP) on biogas conversion of sewage sludge. Water Res. 115, 220–228. https://doi.org/10.1016/j.watres.2017.02.064.

Dong, B., Xia, Z., Sun, J., Dai, X., Chen, X., Ni, B.J., 2019. The inhibitory impacts of nano-graphene oxide on methane production from waste activated sludge in anaerobic digestion. Sci. Total Environ. 646, 1376–1384. https://doi.org/10.1016/j.scitotenv.2018.07.424.

Falås, P., Wick, A., Castronovo, S., Habermacher, J., Ternes, T.A., Joss, A., 2016. Tracing the limits of organic micropollutant removal in biological wastewater treatment. Water Res. 95, 240–249. https://doi.org/10.1016/j.watres.2016.03.009.

Feng, L., Casas, M.E., Ottosen, L.D.M., Møller, H.B., Bester, K., 2017. Removal of antibiotics during the anaerobic digestion of pig manure. Sci. Total Environ. 603–604, 219–225. https://doi.org/10.1016/j.scitotenv.2017.05.280.

Golet, E.M., Xifra, I., Siegrist, H., Alder, A.C., Giger, W., 2003. Environmental exposure assessment of fluoroquinolone antibacterial agents from sewage to soil. Environ. Sci. Technol. 37 (15), 3243–3249. https://doi.org/10.1021/es0264448.

Gómez, M.J., Martínez Bueno, M.J., Lacorte, S., Fernández-Alba, A.R., Agüera, A., 2007. Pilot survey monitoring pharmaceuticals and related compounds in a sewage treatment plant located on the Mediterranean coast. Chemosphere 66 (6), 993–1002. https://doi.org/10.1016/j.chemosphere.2006.07.051.

Gonzalez-Gil, L., Carballa, M., Lema, J.M., 2017. Cometabolic enzymatic transformation of organic micropollutants under methanogenic conditions. Environ. Sci. Technol. 51 (5), 2963–2971. https://doi.org/10.1021/acs.est.6b05549.

Gros, M., Marti, E., Balcázar, J.L., Boy-Roura, M., Busquets, A., Colón, J., Sànchez-Melsió, A., Lekunberri, I., Borrego, C.M., Ponsá, S., Petrovic, M., 2019a. Fate of pharmaceuticals and antibiotic resistance genes in a full-scale on-farm livestock waste treatment plant. J. Hazard Mater. 378, 120716 https://doi.org/10.1016/j.jhazmat.2019.05.109.

Gros, M., Mas-Pla, J., Boy-Roura, M., Geli, I., Domingo, F., Petrović, M., 2019b. Veterinary pharmaceuticals and antibiotics in manure and slurry and their fate in amended agricultural soils: findings from an experimental field site (Baix Empordà, NE Catalonia). Sci. Total Environ. 654, 1337–1349. https://doi.org/10.1016/j.scitotenv.2018.11.061.

Johnravindar, D., Liang, B., Fu, R., Luo, G., Meruvu, H., Yang, S., Yuan, B., Fei, Q., 2020. Supplementing granular activated carbon for enhanced methane production in anaerobic co-digestion of post-consumer substrates. Biomass Bioenergy 136, 105543. https://doi.org/10.1016/j.biombioe.2020.105543.

Kümmerer, K., 2009. The presence of pharmaceuticals in the environment due to human use - present knowledge and future challenges. J. Environ. Manag. 90 (8), 2354–2366. https://doi.org/10.1016/j.jenvman.2009.01.023.

Lahti, M., Oikari, A., 2010. Microbial Transformation of Pharmaceuticals Naproxen , Bisoprolol , and Diclofenac in Aerobic and Anaerobic Environments, pp. 202–210. https://doi.org/10.1007/s00244-010-9622-2, 61(2).

Lee, J.Y., Lee, S.H., Park, H.D., 2016. Enrichment of specific electro-active microorganisms and enhancement of methane production by adding granular activated carbon in anaerobic reactors. Bioresour. Technol. 205, 205–212. https://doi.org/10.1016/j.biortech.2016.01.054.

Li, Y., Zhang, Y., Liu, Y., Zhao, Z., Zhao, Z., Liu, S., Zhao, H., Quan, X., 2016. Enhancement of anaerobic methanogenesis at a short hydraulic retention time via bioelectrochemical enrichment of hydrogenotrophic methanogens. Bioresour. Technol. 218, 505–511. https://doi.org/10.1016/j.biortech.2016.06.112.

Lin, K., Gan, J., 2011. Sorption and degradation of wastewater-associated non-steroidal anti-inflammatory drugs and antibiotics in soils. Chemosphere 83 (3), 240–246. https://doi.org/10.1016/j.chemosphere.2010.12.083.

Lin, R., Cheng, J., Zhang, J., Zhou, J., Cen, K., Murphy, J.D., 2017. Boosting biomethane yield and production rate with graphene: the potential of direct interspecies electron transfer in anaerobic digestion. Bioresour. Technol. 239, 345–352. https://doi.org/10.1016/j.biortech.2017.05.017.

Liu, Y., Wang, Q., Zhang, Y., Ni, B.J., 2015. Zero valent iron significantly enhances methane production from waste activated sludge by improving biochemical methane potential rather than hydrolysis rate. Sci. Rep. 5, 1–6. https://doi.org/10.1038/srep08263.

Muratçobanoğlu, H., Begüm Gökçek, Ö., Muratçobanoğlu, F., Mert, R.A., Demirel, S., 2022. Biomethane enhancement using reduced graphene oxide in anaerobic digestion of municipal solid waste. Bioresour. Technol. 354, 127163 https://doi.org/10.1016/j.biortech.2022.127163.

Narumiya, M., Nakada, N., Yamashita, N., Tanaka, H., 2013. Phase distribution and removal of pharmaceuticals and personal care products during anaerobic sludge digestion. J. Hazard Mater. 260, 305–312. https://doi.org/10.1016/j.jhazmat.2013.05.032.

Ponzelli, M., Radjenovic, J., Drewes, J.E., Koch, K., 2022. Enhanced methane production kinetics by graphene oxide in fed-batch tests. Bioresour. Technol. 360, 127642 https://doi.org/10.1016/j.biortech.2022.127642.

Rotaru, A.E., Woodard, T.L., Nevin, K.P., Lovley, D.R., 2015. Link between capacity for current production and syntrophic growth in Geobacter species. Front. Microbiol. 6, 744. https://doi.org/10.3389/fmicb.2015.00744.

Schloss, P.D., Westcott, S.L., Ryabin, T., Hall, J.R., Hartmann, M., Hollister, E.B., Lesniewski, R.A., Oakley, B.B., Parks, D.H., Robinson, C.J., Sahl, J.W., Stres, B., Thallinger, G.G., Van Horn, D.J., Weber, C.F., 2009. Introducing mothur: open-source, platform-independent, community-supported software for describing and comparing microbial communities. Appl. Environ. Microbiol. 75 (23), 7537–7541. https://doi.org/10.1128/AEM.01541-09.

Senta, I., Matošić, M., Jakopović, H.K., Terzic, S., Ćurko, J., Mijatović, I., Ahel, M., 2011. Removal of antimicrobials using advanced wastewater treatment. J. Hazard Mater. 192 (1), 319–328. https://doi.org/10.1016/j.jhazmat.2011.05.021.

Spongberg, A.L., Witter, J.D., 2008. Pharmaceutical compounds in the wastewater process stream in Northwest Ohio. Sci. Total Environ. 397 (1–3), 148–157. https://doi.org/10.1016/j.scitotenv.2008.02.042.

Subirats, J., Royo, E., Balcázar, J.L., Borrego, C.M., 2017. Real-time PCR assays for the detection and quantification of carbapenemase genes (bla KPC, bla NDM, and bla OXA-48) in environmental samples. Environmental Science and Pollution Research 24 (7), 6710–6714. https://doi.org/10.1007/s11356-017-8426-6.

Summers, Z.M., Fogarty, H.E., Leang, C., Franks, A.E., Malvankar, N.S., Lovley, D.R., 2010. Direct exchange of electrons within aggregates of an evolved syntrophic coculture of anaerobic bacteria. Science 330 (6009), 1413–1415. https://doi.org/10.1126/science.1194472.

Wang, D., Wang, G., Zhang, G., Xu, X., Yang, F., 2013. Using graphene oxide to enhance the activity of anammox bacteria for nitrogen removal. Bioresour. Technol. 131, 527–530. https://doi.org/10.1016/j.biortech.2013.01.099.

Wang, G., Xu, X., Yang, F., Zhang, H., Wang, D., 2014. Using graphene oxide to reactivate the anaerobic ammonium oxidizers after long-term storage. J. Environ. Chem. Eng. 2 (2), 974–980. https://doi.org/10.1016/j.jece.2014.03.014.

Wang, P., Zheng, Y., Lin, P., Li, J., Dong, H., Yu, H., Qi, L., Ren, L., 2021. Effects of graphite, graphene, and graphene oxide on the anaerobic co-digestion of sewage sludge and food waste: attention to methane production and the fate of antibiotic resistance genes. Bioresour. Technol. 339 (June), 125585 https://doi.org/10.1016/j.biortech.2021.125585.

Wei, X.L., Ge, Z.Q., 2013. Effect of graphene oxide on conformation and activity of catalase. Carbon 60, 401–409. https://doi.org/10.1016/j.carbon.2013.04.052.

Wrighton, K.C., Agbo, P., Warnecke, F., Weber, K.A., Brodie, E.L., DeSantis, T.Z., Hugenholtz, P., Andersen, G.L., Coates, J.D., 2008. A novel ecological role of the Firmicutes identified in thermophilic microbial fuel cells. ISME J. 2 (11), 1146–1156. https://doi.org/10.1038/ismej.2008.48.

Wu, Y., Wang, S., Liang, D., Li, N., 2020. Conductive materials in anaerobic digestion: from mechanism to application. Bioresour. Technol. 298 https://doi.org/10.1016/j.biortech.2019.122403. November 2019.

Xu, S., He, C., Luo, L., Lü, F., He, P., Cui, L., 2015. Comparing activated carbon of different particle sizes on enhancing methane generation in upflow anaerobic digester. Bioresour. Technol. 196, 606–612. https://doi.org/10.1016/j.biortech.2015.08.018.

Xu, W., Zhang, G., Li, X., Zou, S., Li, P., Hu, Z., Li, J., 2007. Occurrence and elimination of antibiotics at four sewage treatment plants in the Pearl River Delta (PRD), South China. Water Res. 41 (19), 4526–4534. https://doi.org/10.1016/j.watres.2007.06.023.

Xu, Y., Wang, M., Yu, Q., Zhang, Y., 2020. Enhancing methanogenesis from anaerobic digestion of propionate with addition of Fe oxides supported on conductive carbon cloth. Bioresour. Technol. 302, 122796 https://doi.org/10.1016/j.biortech.2020.122796.

Xue, W., Wu, C., Xiao, K., Huang, X., Zhou, H., Tsuno, H., Tanaka, H., 2010. Elimination and fate of selected micro-organic pollutants in a full-scale anaerobic/anoxic/aerobic process combined with membrane bioreactor for municipal wastewater reclamation. Water Res. 44 (20), 5999–6010. https://doi.org/10.1016/j.watres.2010.07.052.

Yun, H., Liang, B., Ding, Y., Li, S., Wang, Z., Khan, A., Zhang, P., Zhang, P., Zhou, A., Wang, A., Li, X., 2021. Fate of antibiotic resistance genes during temperature-changed psychrophilic anaerobic digestion of municipal sludge. Water Res. 194, 116929 https://doi.org/10.1016/j.watres.2021.116926.

Zahedi, S., Gros, M., Balcazar, J.L., Petrovic, M., Pijuan, M., 2021. Assessing the occurrence of pharmaceuticals and antibiotic resistance genes during the anaerobic treatment of slaughterhouse wastewater at different temperatures. Sci. Total Environ. 789, 147910 https://doi.org/10.1016/j.scitotenv.2021.147910.

Zahedi, S., Romero-Güiza, M., Icaran, P., Yuan, Z., Pijuan, M., 2018. Optimization of free nitrous acid pre-treatment on waste activated sludge. Bioresour. Technol. 252, 216–220. https://doi.org/10.1016/j.biortech.2017.12.090. November 2017.

Zhang, J., Wang, Z., Wang, Y., Zhong, H., Sui, Q., Zhang, C., Wei, Y., 2017. Effects of graphene oxide on the performance, microbial community dynamics and antibiotic resistance genes reduction during anaerobic digestion of swine manure. Bioresour. Technol. 245, 850–859. https://doi.org/10.1016/j.biortech.2017.08.217.

Zhang, R., Gu, J., Wang, X., Li, Y., Liu, J., Lu, C., Qiu, L., 2019. Response of antibiotic resistance genes abundance by graphene oxide during the anaerobic digestion of swine manure with copper pollution. Sci. Total Environ. 654, 292–299. https://doi.org/10.1016/j.scitotenv.2018.11.094.

Zhang, R., Li, J., Zhou, L., Zhuang, H., Shen, S., Wang, Y., 2022. Effect of graphene and graphene oxide on antibiotic resistance genes during copper - contained swine manure anaerobic digestion. Environ. Sci. Pollut. Control Ser. 1–12. https://doi.org/10.1007/s11356-022-23741-y.

Zou, W., Li, X., Lai, Z., Zhang, X., Hu, X., Zhou, Q., 2016. Graphene oxide inhibits antibiotic uptake and antibiotic resistance gene propagation. ACS Appl. Mater. Interfaces 8 (48), 33165–33174. https://doi.org/10.1021/acsami.6b09981.